Journal of
*Marine Science and Engineering*

MDPI

*Article*

# Formation Transformation Method for UUV Group to Approach a Static Target

**Liangang Yin [1], Zheping Yan [2] and Yunzhi Hou [3,*]**

[1] College of Intelligent Systems Science and Engineering, Harbin Engineering University, Harbin 150001, China; noseccond@163.com
[2] Qingdao Innovation and Development Center, Harbin Engineering University, Qingdao 266000, China; yanzheping@hrbeu.edu.cn
[3] Denso Shanghai Smart Mobility Technology Company, Ltd., Xi'an Branch, Xi'an 710075, China
* Correspondence: hyunzh@126.com

**Abstract:** The unmanned underwater vehicle (UUV) group composed of UUVs carrying different kinds of detection equipment is powerful for underwater target searching and detection. In this paper, a formation transformation method, used while the mission of the UUV group transformed from searching to detecting, is proposed. Firstly, a new formation transformation strategy, in which the UUVs converged to their detection points followed by the aggregation points achieved, is proposed to improve the safety of UUVs during transformation. Following the proposed strategy, particle swarm optimization is employed to find the optimal aggregation points. Finally, possible collisions between UUVs and collisions between UUVs and targets are avoided by adding a collision avoidance algorithm based on a virtual torque field. The model prediction is used to solve the delay problem of underwater communication, and the communication results are used to correct the model prediction results. The test shows that the method is effective. The effectiveness of the proposed method is demonstrated using two simulation examples.

**Keywords:** unmanned underwater vehicle group; formation transformation; collision avoidance



**Citation:** Yin, L.; Yan, Z.; Hou, Y. Formation Transformation Method for Searching UUV Group to Approach a Static Target. *J. Mar. Sci. Eng.* **2023**, *11*, 2030. https://doi.org/10.3390/jmse11102030

Academic Editor: Alessandro Ridolfi

Received: 25 September 2023
Revised: 15 October 2023
Accepted: 19 October 2023
Published: 23 October 2023



## 1. Introduction

Marine development has contributed to the development of marine development tools. Underwater unmanned vehicles (UUVs) have become an important tool for marine exploitation due to their low cost, low risk and excellent performance [1]. As an auxiliary intelligent tool for marine exploration, UUVs have been extensively employed in military and civil fields such as submarine reconnaissance, anti-submarine patrol, emergency search and rescue, marine environmental mapping, resource exploration and so on [2–4]. Thus, they have become a research hotspot for marine scientists. However, with the increasing complexity of military requirements and the expansion of exploration of sea areas, it is almost impossible to rely solely on an individual UUV to complete tasks independently. In addition, an individual UUV is faced with the limitations of poor redundancy, small mission scope and low work efficiency. It is difficult for an individual UUV to meet the requirements of underwater tasks in complex marine environments. UUV groups are more efficient and fault-tolerant than individual UUVs, and they can perform more complex tasks [5]. Overall, UUV groups cooperate with each other to perform tasks, which has become the mainstream direction of underwater vehicle research.

Formation coordination ability [6,7] is necessary for UUV groups to perform tasks. Although the research on formation coordination control of UUVs started late, it has great potential in practical applications [8–10]. In the civil scope, the formation coordination ability of UUV groups can help to complete large-scale sea area hydrological surveys and chart calibration. In industrial applications, the formation coordination ability of UUV groups can help to complete the laying, regular inspection and maintenance of subsea oil and gas pipelines. In military applications, the formation coordination ability of UUV groups can help to cooperate to complete the detection of minefields and mine clearance; cooperate to complete naval intelligence reconnaissance and dangerous area surveillance; and cooperate to block enemy ports over a large area to improve the hit rate and operational efficiency of attacking enemy targets, which is of great military significance. It is worth mentioning that the ability of formation transformation is the embodiment of the formation coordination ability of a UUV group [11]. Formation transformation plays an important role in obstacle avoidance and containment of moving targets. Underwater target detection is an important application direction for UUV groups. Generally, only one type of detection equipment is used by a UUV group during an underwater target detection mission. The widely used sonar can acquire hydroacoustic images of the underwater environment. It has a long detection range, but the resolution of hydroacoustic images is low [12]. The detection range of an underwater camera is small, but its image has high resolution. A variety of features of underwater targets are analyzed from images [13]. When sonar detects a target that cannot be accurately identified, the UUV group can change formation to use underwater cameras for further detection. The formation transformation ability of a UUV group organically combines the two devices, so that the underwater target detection ability can be improved.

The method of achieving formation transformation is to combine a formation transformation strategy with a formation coordination algorithm. Formation coordination methods include the leader–follower method [14], virtual structure method [15], model prediction method [16], artificial potential field method [17] and consensus method [18], etc. Therein, the basic idea of the leader–follower method [19] is to divide the UUVs in the UUV group into two categories, and designate a certain UUV as the active leader, and other UUVs as passive followers. The leader can control the movement trend of the entire UUV group system by executing a preset movement trajectory, and each follower can realize the formation control by maintaining a certain distance and azimuth constraints from the leader. The leader–follower method can achieve the purpose of controlling the behavior of the entire UUV group only by giving the trajectory of the leader UUV. Therefore, its formation control structure is simple and its application is very extensive. The core idea of the virtual structure method [20] is that each UUV matches its own expected motion according to the motion characteristics of the virtual structure, and finally determines its own motion path. Therefore, in order to realize the virtual structure, it is necessary to first define the dynamic characteristics of the ideal virtual structure, then convert the motion of the virtual structure into the desired motion of the virtual target point, and finally derive the control law of the UUV tracking the corresponding virtual target point on the virtual structure, so as to realize the formation. The virtual structure method is convenient to determine the formation behavior of the entire UUV group, but it lacks flexibility and adaptability. The basic idea of the artificial potential field method is to construct the virtual potential field force (attraction and repulsion force) between UUVs, between UUVs and targets, as well as between UUVs and obstacles in the formation by setting the artificial potential field and potential field function, and then obtain the control input of each UUV. The advantage of the artificial potential field method is that the algorithm design is intuitive and effective, the calculation is simple, and it is easy to realize real-time control. It can effectively deal with the obstacle avoidance problem, especially under the constraint of obstacles. The disadvantage is that there is a problem of local minimum, and it is difficult to design a suitable potential field function. Additionally, it deserves to be mentioned that NOGUCHI Y et al. [21] proposed an artificial potential field based on a binary Bayesian filter for path planning. BECHLIOULIS C P et al. [22] proposed a decentralized control protocol with minimal complexity to solve the distance-based formation control problem of multiple autonomous underwater vehicles in a leader–follower architecture. FUADY S et al. [23] solved the problem of distributed formation control with obstacle avoidance using the consensus method and designed a formation center estimator for the consensus algorithm. ZHANG S et al. [24] combined consensus with the leader–follower method to design a formation control algorithm. XING W et al. [25,26] designed a consensus control strategy based on event-triggered communication and pinning control for multi-agent systems subject to network-induced time-varying delays, parametric uncertainties and external disturbances.

In the process of formation transformation, the ability to avoid obstacles is essential for the UUV group [27–29]. This is due to the lack of prior knowledge of the environment in the process of UUV group performing tasks, so obstacles may appear in the path planned in advance. UUVs need to plan the path in real time to avoid obstacles, and also avoid collision with other UUVs owing to route change. In addition, the distance between UUVs cannot be too far, otherwise the communication between UUVs may be affected, and even the formation cannot be restored after obstacle avoidance. Therefore, in order to ensure the safety of UUVs and the normal execution of subsequent tasks. UUVs need to cooperate with each other to avoid obstacles while taking into account the formation requirements [30]. Because each UUV in the UUV group is constrained by the position and formation of obstacles, it is more difficult to deal with the problem of multiple UUVs' cooperative obstacle avoidance. At present, many scholars have carried out in-depth research on UUV group cooperative obstacle avoidance based on formation control methods. For example, Wang L L et al. [31] solved the problem of collision avoidance control of multi-AUV time-varying formation system by using the fixed-time event-triggered obstacle avoidance consensus control. ZHANG W et al. [32] converted the attractive force of the target and the repulsive force of the obstacle to potential field strength. The traditional vector force control is replaced by the method of potential field strength. LIU Y et al. [33] designed an optimized potential field function, then obtained the obstacle avoidance method according to the gradient of the potential field function and coordinate input.

In this paper, the formation transformation strategy of aggregation followed by convergence is proposed. Achieving their aggregation points in advance, the UUVs could gradually converge to their desired positions safely. To further improve the efficiency and safety of the formation transformation, the aggregation points are optimized by the particle optimization algorithm. In addition, a new avoidance method, in which a virtual torque field is constructed to enforce the UUVs changing their original directions, is proposed to improve the safety of UUVs during formation transformation.

This paper is organized as follows. In Section 2, a new formation transformation strategy with particle swarm optimization is proposed to improve the safety of UUVs during transformation. In Section 3, a collision avoidance algorithm based on a virtual torque field is introduced to avoid the possible collisions between UUVs and collisions between UUVs and targets. In Section 4, two examples are used to illustrate the effectiveness of the proposed approach. Section 5 concludes the research in this article.

## 2. Formation Transformation Strategy

### *2.1. Formation Transformation Strategy*

Normally, UUV groups would keep a formation with higher search efficiency while carrying out the initial screening task. However, due to the limited resolution of sonar, it is often challenging to determine the exact properties of these targets. To enhance the UUVs' detection capabilities and address the issue of unclear target identification, the UUV group gradually narrows its formation, approaches suspected targets to form a new configuration and employs its onboard underwater cameras for further target investigation. A common formation transformation process is shown in Figure 1, where a frequently used formation for detection is formed by a circle centered on the suspected target. It has a enough small radius to ensure the UUVs are close enough to the suspected target for high measurement accuracy.

A small detection formation radius means that the UUVs move close to each other and the suspected target during the transformation progress. To improve safe distances of UUVs from other UUVs and the suspected target, the formation transformation strategy is proposed as follows. To each of the $UUV_i$ final detection points, assign an aggregation point, and enforce the UUVs to achieve their corresponding aggregation points before continuing to their final detection points. The aggregation points and detection points are evenly distributed on two circles of radii $\delta_{Od}$ and $r_d$ with same center located at the suspected target $O$. Moreover, the corresponding aggregation points, detection points and the suspected target are in the same line, shown as the pink and blue point in Figure 2.

Once a suspected target is found, UUVs gradually gather to the aggregation points from the original loose search formation. To ensure smooth underwater communication, the UUV group needs to maintain a consistent depth underwater. In the detection of stationary targets, the emphasis is on the target depth, through the formation control of UUVs close to the target, so 2D formation control is the research object of this paper. During this procedure, an avoidance strategy should be active to ensure the safety of UUVs. As the UUVs reach their corresponding aggregation points, the avoidance strategy can be switched off and the UUVs are further concentrated towards their detection points. Ultimately, the UUV group completes its formation transformation from a loose search one to a dense detection one. With the aggregation points introduced, the proposed formation transformation strategy can improve safety of the UUVs and lower the requirements of the avoidance strategy.

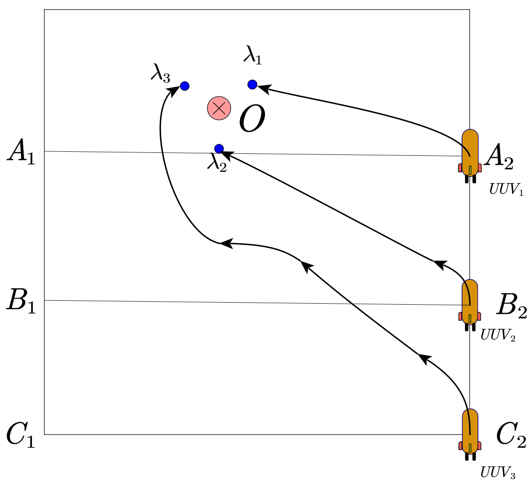


**Figure 1.** Formation transformation.

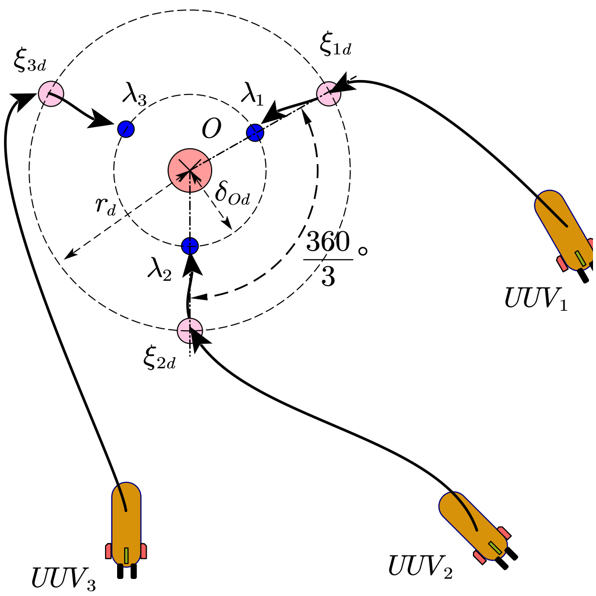


**Figure 2.** Transformation with new strategy.

### 2.2. Optimization of Aggregation Points

Firstly, define the specific distribution of aggregation points based on the transformation strategy, as shown in Figure 3. Because the angles between the aggregation points are fixed, when $\theta_1$ changes, the positions of the other points also move along the circle. $\theta_1$ and $r_d$ will affect the intersection points of UUV paths and the time it takes for UUVs to reach the aggregation points. Selecting the appropriate aggregation points is part of the research in this paper.

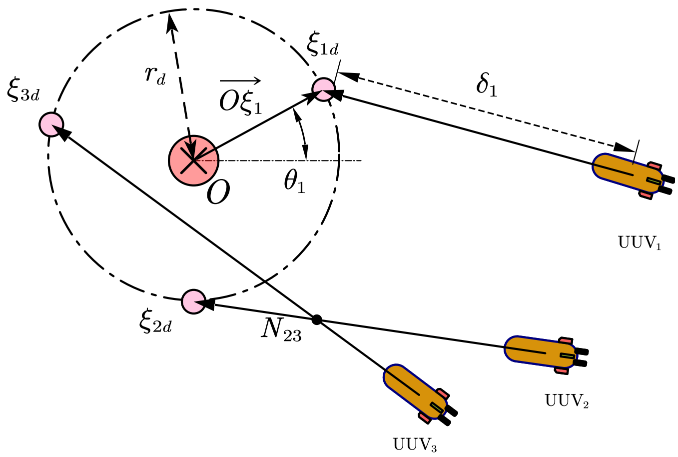


**Figure 3.** Location distribution of UUVs and aggregation points.

When there are three UUVs, there are two distribution relations $s_1$ and $s_2$ in counterclockwise direction, which are $\xi_{1d} \to \xi_{2d} \to \xi_{3d} \to \xi_{1d}$ and $\xi_{1d} \to \xi_{3d} \to \xi_{2d} \to \xi_{1d}$.

This paper utilizes the particle swarm optimization algorithm to determine the optimal aggregation point. The selection of the objective function considers the following main factors: the distance between UUVs and the aggregation point; the time difference for each UUV to reach the aggregation point; and the intersection of paths to the aggregation point.

The position distribution of the aggregation points needs to satisfy the requirements of group safety and coordination. Firstly, the maximum distance $\delta_{max}$ between UUVs and the aggregation point should be minimized. This aims to ensure that the UUVs arrive at the target location as close together in time as possible, that is, the distance between each UUV and the target position is as close as possible. Currently, the standard deviation $\sigma_{dis}$ of the distance between the UUV and the target is small. In order to ensure that the time for UUV to reach the target position is as close as possible, the distance between UUV and the target position should be as close as possible, so the standard deviation $\bar{\delta}$ between UUV and the target point should be smaller. To reduce the possibility of UUV collisions, it is desirable to minimize the number of intersection points $N_c$. All three factors are considered equally important. Therefore, the optimization function is defined as follows:

$$f = \sigma_{dis} + \delta_{\max} + \bar{\delta} N_c \tag{1}$$

where $N_c$ is multiplied by $\bar{\delta}$ so that the expression before the equal sign is of the same order of magnitude as the expression after the equal sign.

Once the initial positions of the UUVs are determined, $\bar{\delta}$ , $\sigma_{dis}$, $N_c$ and $\bar{\delta}$ are functions of $\theta_1$ and $r_d$ . Thus, the optimization objective function can be abstracted as follows:

$$f = f_{target}(\theta_1, r_d) \tag{2}$$

Next, the particle algorithm is utilized to obtain the optimal values of $\theta_1$ and $r_d$.

**The optimization simulation case:** The initial positions of UUVs and the suspected target are shown in Table 1.

The variation of the objective function values for the two distributions of target points $s_1$ ($\xi_{1d} \to \xi_{2d} \to \xi_{3d} \to \xi_{1d}$) and $s_2$ ($\xi_{1d} \to \xi_{3d} \to \xi_{2d} \to \xi_{1d}$) in Section 2.2 is shown in Figure 4:

**Table 1.** The initial positions of UUVs and the suspected target.

| **Number** | $x$ **(m)** | $y$ **(m)** |
|---|---|---|
| $UUV_1$ | 400 | 50 |
| $UUV_2$ | 550 | 150 |
| $UUV_3$ | 500 | 50 |
| $O$ | 300 | 300 |

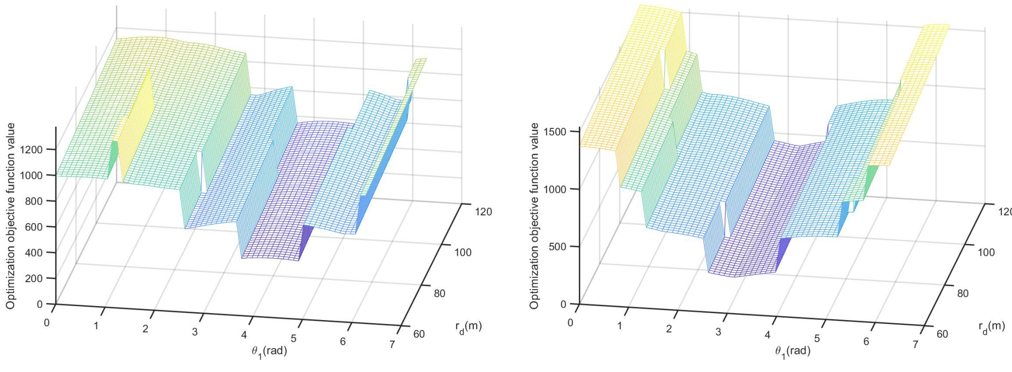


(**a**) (**b**)

**Figure 4.** Function value surface. (**a**) Distribution $s_1$. (**b**) Distribution $s_2$.

Particle optimization results for the two distribution cases are shown in Figure 5:

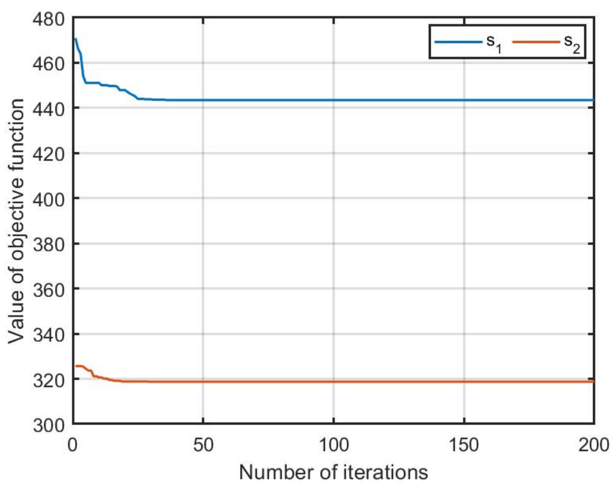


**Figure 5.** The convergence curve of the optimized objective function.

In this simulation case, the convergence curve displays that the value of the optimization objective function converges to the stable value quickly. The optimization objective function has a smaller value at $s_2$, the minimum value of which is 318.7, the corresponding optimal solutions are $\theta_1 = 179.04°$ and $r_d = 60.0$ m.

Compared with directly setting the formation change of the desired position, the optimization of the location of the aggregation point comprehensively considers the security of the UUV and the efficiency of the formation transformation, rather than focusing on one side.

## 3. The Avoidance Method Based on Virtual Forces

### 3.1. UUV Motion Model

Firstly, the UUV motion model is established and simplified, only considering the motion of surge, sway, and yaw in the horizontal plane. The simplified UUV motion model with three degrees of freedom is as follows:

$$\begin{cases} \dot{\eta} = J(\eta)v \\ M\dot{v} + C(v)v + Dv = \tau_c \end{cases} \tag{3}$$

where $J(\eta)$ is the Jacobian matrix; $M$ is the inertia matrix; $C(v)$ is the Coriolis and centripetal forces; $D$ represents the damping matrix. $D$ typically represents the damping matrix, used to describe the damping forces acting on the object, and it does not include hydrodynamic parameters. Hydrodynamic parameters are usually included in other parts of the equation, such as the mass matrix $M$ and the Coriolis matrix $C(v)$. $\eta = [x, y, \psi]^{\mathrm{T}}$ is the state information of the position and Euler angles; $v = [u, v, r]^{\mathrm{T}}$ is the state information of velocities; $\tau_c$ is the fully driven UUV control input force and torque. The dynamic part in Equation (3) is written as equations as follows:

$$\begin{cases} \dot{u} = \frac{m_{22}}{m_{11}}vr - \frac{X_u}{m_{11}}u - \frac{X_{u|u|}}{m_{11}}u|u| + \frac{1}{m_{11}}\tau_x \\ \dot{v} = -\frac{m_{11}}{m_{22}}ur - \frac{Y_v}{m_{22}}v - \frac{Y_{v|v|}}{m_{22}}v|v| + \frac{1}{m_{22}}\tau_y \\ \dot{r} = \frac{m_{11}-m_{22}}{m_{33}}ur - \frac{N_r}{m_{33}}r - \frac{N_{r|r|}}{m_{33}}r|r| + \frac{1}{m_{33}}\tau_r \end{cases} \tag{4}$$

where $m_{ii}$, $X_u$, $X_{u|u|}$, $Y_v$, $Y_{v|v|}$, $N_r$ and $N_{r|r|}$ represent the hydrodynamic coefficients, and they are all greater than 0.

### 3.2. Consensus Control for Distance to the Target

To coordinate the motion state of the UUV group in the formation transformation, a consensus method is used to make the UUVs reach the gathering point together.

Decompose the UUV and the directed line segment formed by the desired position into two scalars: the distance from the desired position and the desired heading. By controlling the heading to track the desired heading, achieving consistency in the distance between the UUV group and the desired position is sufficient to achieve positional consistency. So the complex linearization process of location consistency is omitted.

Assuming that there are n UUVs in the group, according to the UUV longitudinal second-order nonlinear longitudinal motion model in Equation (4), it is rewritten in the following form:

$$\begin{cases} \dot{l}_i = u_i \\ \dot{u}_i = f_i(u_i, v_i, r_i) + \tau_{xi} \end{cases} \quad i \in \{1, \ldots, n\} \tag{5}$$

where $l_i$ is the distance of UUV$_i$ from the desired position, and $l_i \leq 0$, $u_i, v_i, r_i$ are the longitudinal velocity, lateral velocity, and angular velocity of UUV$_i$, $\tau_{xi}$ is the longitudinal control input and $f_i(u_i, v_i, r_i)$ is the nonlinear term in the longitudinal motion model.

For the second-order nonlinear model of a UUV, a consistency control protocol is constructed as follows:

$$\tau_{xi} = -k_{x1}u_i - k_{x2}l_i - k_{x3}\sum_{j=1}^{n} a_{ij}(l_i - l_j) \tag{6}$$

where $k_{xi}$ denotes the control gain and is always positive. $a_{ij}$ is the connection weight between communication topology nodes, and the weight is non-negative.

**Definition 1.** *For any initial condition $l_0$ and $v_0$, if the following condition is satisfied,*

$$\begin{cases} \lim\limits_{t\to\infty} |l_i(t) - l_j(t)| = 0 \\ \lim\limits_{t\to\infty} |u_i(t) - u_j(t)| = 0 \end{cases} \quad i \in \{1, \ldots, n\} \tag{7}$$

*then the UUV group can achieve consensus.*

Algebraic graph theory is an important tool for describing the information interaction among intelligent agents. The topological communication graph is mainly composed of nodes, edges connecting nodes and connection weights. In this paper, the communication topological graph of the UUV group is assumed to be an undirected graph, which means that there is always an undirected path connecting any two different nodes.

**Assumption 1.** *The communication topological graph of the UUV group is undirected and connected, and they communicate with each other with the same weight.*

**Assumption 2.** *For the nonlinear term in Equation (5), there always exists a constant such that the nonlinear term satisfies the following inequality,*

$$|f_i(u_i, v_i, r_i)| \leq \omega_i |u_i| \tag{8}$$

**Theorem 1.** *Under the Assumption 1 that the UUV group communication topological graph is an undirected connected graph and satisfies Assumption 2, then under the consistency control protocol (3–14), if the speed control gain satisfies the following inequality:*

$$\omega_i \leq k_{x1}, i = 1, \ldots, n \tag{9}$$

*then the UUV group can ultimately achieve longitudinal consistency.*

**Proof.** Under the control protocol Equation (7), the UUV longitudinal second-order nonlinear dynamic model can be written as

$$\begin{cases} \dot{l}_i = u_i \\ \dot{u}_i = f_1(u_i, v_i, r_i) - k_{x1} u_i - k_{x2} l_i - k_{x3} \sum_{j=1}^{n} a_{ij} (l_i - l_j) \end{cases} \quad i \in \{1, \ldots, n\} \tag{10}$$

□

Construct the following Lyapunov function:

$$V = V_1 + V_2 \tag{11}$$

$$V_1 = \frac{1}{2} k_{x3} \sum_{i=1}^{n} \sum_{j=1}^{n} a_{ij} (l_i - l_j)^2 + k_{x2} \sum_{i=1}^{n} l_i^2 \tag{12}$$

$$V_2 = \sum_{i=1}^{n} u_i^2 \tag{13}$$

Obviously, the Lyapunov function $V$ is positive definite.
Taking the derivative, we obtain

$$\dot{V}_1 = k_{x3} \sum_{i=1}^{n} \sum_{j=1}^{n} a_{ij} \left(l_i - l_j\right) \left(u_i - u_j\right) + 2k_{x2} \sum_{i=1}^{n} l_i u_i \tag{14}$$

From Assumption 1, the adjacency matrix $A \in R^{n\times n}$ of the element $a_{ij}$ is a symmetric matrix, that is $a_{ij} = a_{ji}$, hence

$$\sum_{i=1}^{n}\sum_{j=1}^{n} a_{ij}(l_i - l_j)u_i = -\sum_{i=1}^{n}\sum_{j=1}^{n} a_{ij}(l_i - l_j)u_j \tag{15}$$

Therefore, Equation (14) can be written as follows:

$$\dot{V}_1 = 2k_{x3}\sum_{i=1}^{n}\sum_{j=1}^{n} a_{ij}u_i(l_i - l_j) + 2k_{x2}\sum_{i=1}^{n} l_i u_i \tag{16}$$

Then, take the derivative of $V_2$ and obtain

$$\dot{V}_2 = 2\sum_{i=1}^{n} u_i\dot{u}_i \tag{17}$$

Combining Equation (10), Equation (17) can be written as

$$\begin{aligned}\dot{V}_2 &= 2\sum_{i=1}^{n} u_i \cdot \left[f_1(u_i, v_i, r_i) - k_{x1}u_i - k_{x2}l_i - k_{x3}\sum_{j=1}^{n} a_{ij}(l_i - l_j)\right] \\ &= 2\sum_{i=1}^{n} u_i f_1(u_i, v_i, r_i) - 2k_{x3}\sum_{i=1}^{n}\sum_{j=1}^{n} a_{ij}u_i(l_i - l_j) - \\ &\quad 2k_{x1}\sum_{i=1}^{n} {u_i}^2 - 2k_{x2}\sum_{i=1}^{n} u_i l_i\end{aligned} \tag{18}$$

Combining Equations (16) and (18), $\dot{V}$ can be written as

$$\dot{V} = \dot{V}_1 + \dot{V}_2 = 2\sum_{i=1}^{n} u_i f_1(u_i, v_i, r_i) - 2k_{x1}\sum_{i=1}^{n} {u_i}^2 \tag{19}$$

According to Assumption 2, it can be obtained that

$$\begin{aligned}2\sum_{i=1}^{n} u_i f_1(u_i, v_i, r_i) &\le 2\sum_{i=1}^{n} |u_i||f(u_i, v_i, r_i)| \\ &\le 2\sum_{i=1}^{n} \omega_i|u_i||u_i| \le 2\sum_{i=1}^{n} \omega_i u_i^2\end{aligned} \tag{20}$$

Therefore, $\dot{V}$ can be written as follows:

$$\begin{aligned}\dot{V} &= \dot{V}_1 + \dot{V}_2 \\ &\le 2\sum_{i=1}^{n} \omega_i u_i^2 - 2k_{x1}\sum_{i=1}^{n} {u_i}^2 = -2\sum_{i=1}^{n} (k_{x1} - \omega_i)u_i^2\end{aligned} \tag{21}$$

Under condition Equation (9), $\dot{V} \le 0$ , so it can be obtained that

$$\begin{cases}\lim\limits_{t\to\infty} |l_i(t) - l_j(t)| = 0 \\ \lim\limits_{t\to\infty} |u_i(t) - u_j(t)| = 0\end{cases} \quad i \in \{1, \ldots, n\} \tag{22}$$

Then, the UUV group can achieve longitudinal consistency under the control of the consistency control protocol, i.e., the UUVs can reach their respective target points consistently, and the number of UUVs will not affect the consistency and stability. However, when the number increases, the communication volume of each UUV will increase linearly with it.

The paths may cross after the aggregation points are optimized. Therefore, UUVs may collide with each other and UUVs may collide with suspected targets. In order to ensure the safety of the UUV group in the process of formation transformation, UUVs should be able to avoid each other and suspected targets.

In this paper, the virtual torque field is constructed to control UUVs' headings inspired by the virtual force method. The magnitude and direction of the torque is defined according to the position distribution between UUVs and with the obstacles. Assuming that there are no other obstacles in the formation transformation process, the distance between UUVs and the distance between UUVs and the suspected target need to be controlled.

If the distance between two UUVs is less than the avoidance trigger distance, the UUV farther away from the suspected target has more space to avoid another UUV, as shown in Figure 6. When UUV$_j$ avoids UUV$_i$, UUV$_j$ calculates the virtual torque field applied by UUV$_i$ as follows:

$$N_{uij} = \begin{cases} \alpha_{N1}\log(\frac{\delta_{alert}}{\delta_{ij}})(|cos\frac{\theta_{ij}}{2}| + c_{u1}) + c_{u2}, & \delta_{ij} < \delta_{alert} \& \delta_{iO} < \delta_{jO} \& \delta_{ij} \leq \delta_{\min j} \\ 0, & \text{others} \end{cases} \tag{23}$$

where $\alpha_{N1}$ is the virtual torque field strength gain factor; $\delta_{ij}$ is the distance between UUV$_i$ and UUV$_j$; $\delta_{alert}$ is the avoidance trigger distance; $\theta_{ij}$ is the directional angle of UUV$_j$ in the motion coordinate system of UUV$_i$; $\delta_{iO}$ is the distance between UUV$_i$ and the suspected target; $\delta_{\min j}$ is the minimum distance between UUV$_j$ and other UUVs in the group; and $c_{u1}$ and $c_{u2}$ affect the upper and lower limits of the virtual torque field strength.

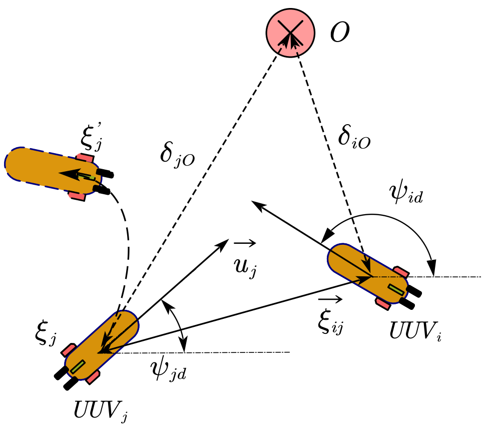


**Figure 6.** The method of avoidance between UUVs.

The position of the suspected target is fixed, and the UUV adjusts its heading to avoid it, as shown in Figure 7. UUV$_j$ calculates the torque field applied by the suspected target based on the distance between them, and the virtual torque field is defined as follows:

$$N_{jO} = \begin{cases} \alpha_{N2}\log(\frac{\delta_{alertO}}{\delta_{jO}}) + c_O, & \delta_{jO} < \delta_{alertO} \& \delta_{jO} < \delta_{\min j} \\ 0, & \text{others} \end{cases} \tag{24}$$

where $\alpha_{N2}$ is the virtual torque field strength gain factor; $\delta_{alertO}$ is the trigger distance for UUVs to avoid the suspected target; $\delta_{jO}$ is the distance between UUV$_j$ and the suspected target; $\delta_{\min O}$ is the minimum distance between other UUVs and the suspected target; and $c_O$ adjusts the upper and lower limits of the virtual torque field strength.

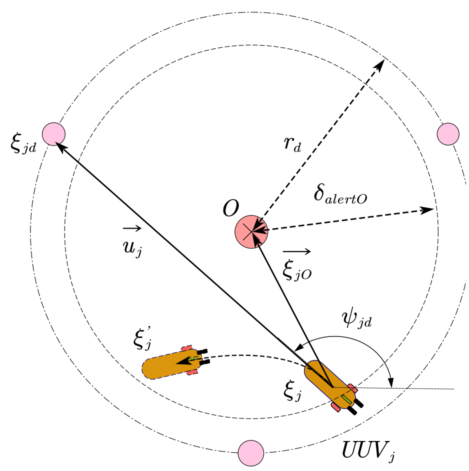


**Figure 7.** The method of UUVs avoiding the suspected target.

If UUV$_i$ and UUV$_j$ need to avoid the suspected target and they need to avoid each other, and UUV$_j$ is closer to the suspected target, then UUV$_j$ avoids the suspected target. Meanwhile, UUV$_i$ adjusts its heading to avoid UUV$_j$ to ensure a safe distance. In this process, in order to avoid UUV$_i$ becoming too close to the suspected target, the avoidance trigger distance $\delta_{alert}$ is larger than $\delta_{alertO}$.

### 3.3. Avoidance Method Based on Virtual Torque Field

The avoidance process of the above two cases is shown in Algorithm 1. The corresponding flow chart is shown in the Figures 8 and 9. It is precisely the torque variations that guide the UUV through the actions outlined in Algorithm 1.

**Algorithm 1** The avoidance algorithm

## The method of avoidance between UUVs.
**if** the distance between two UUVs is less than the avoidance trigger distance and the distance between the two is the smallest **then**
  **if** UUV$_j$ is closer to the suspected target than UUV$_i$ **then**
    calculate the torque field on UUV$_j$ applied by UUV$_i$
  **else**
    calculate the torque field on UUV$_i$ applied by UUV$_j$
  **end if**
**end if**
## The method of UUV to avoid each other and suspected targets
**if** The distance between UUV$_i$ and UUV$_j$ is less than $\delta_{alertO}$ **then**
  **if** UUV$_j$ is closer to the suspected target than UUV$_i$ **then**
    calculates the torque field on UUV$_j$ applied by the suspected target
    calculates the torque field on UUV$_i$ applied by UUV$_j$
  **else**
    UUV$_i$ calculates the torque field applied by the suspected target
    calculate the torque field on UUV$_j$ applied by UUV$_i$
  **end if**
**end if**

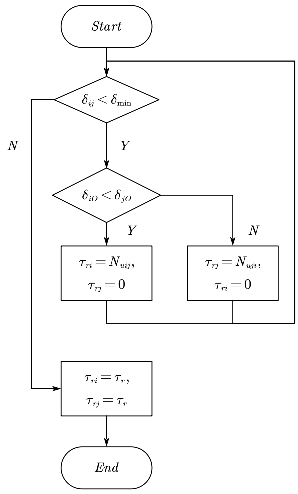


**Figure 8.** The method of avoidance between UUVs.

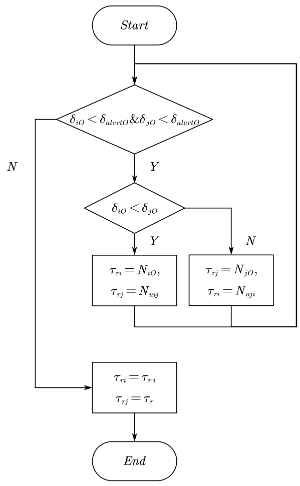


**Figure 9.** The method for UUVs to avoid each other and suspected targets.

The magnitude of the virtual torque field is defined above, and then the direction of the torque is defined. The positive torque causes the UUV rotate counterclockwise, and the negative torque causes the UUV to rotate clockwise. The direction of the torque is given according to the position distribution between UUVs and the position distribution between UUVs and the suspected target. When UUV$_j$ avoids UUV$_i$, the torque is defined as

$$\tau_{rj} = N_{uij}\mathrm{sgn}(\vec{u}_j \times \vec{\xi}_{ji}) \tag{25}$$

where $\vec{u}_j$ is the velocity vector of UUV$_j$; $\vec{\xi}_{ji}$ is the direction vector from UUV$_j$ to UUV$_i$.

When UUV$_j$ avoids the suspected target, the torque is defined as:

$$\tau_{rj} = N_{jO}\mathrm{sgn}(\vec{u}_j \times \vec{\xi}_{jO}) \tag{26}$$

where $\vec{\xi}_{jO}$ is the direction vector from UUV$_j$ to the suspected target, and sgn is a sign function that returns an integer variable indicating the sign (positive or negative) of its parameter.

### *3.4. The Avoidance Speed Control Law*

The virtual torque field is combined with speed control, and this collision avoidance method avoids the problem of falling into the local extremum in the artificial potential field method. The avoidance speed control law is designed to reduce the speed of UUVs and improve the safety of UUVs. When the avoidance action is triggered, UUVs will actively decrease their speed to slow down the approaching trend. The virtual torque field and the avoidance speed control law work together to improve the efficiency and safety of avoidance. The avoidance speed control law is defined as follows:

$$\rho_{ij} = \text{sigmoid}(\frac{\delta_{ij} - 50}{5})\alpha_{u1} + \alpha_{u2} \tag{27}$$

$$\tau_{xi} = \alpha_{u3}\rho_{ij} - \alpha_{u4}u_i \tag{28}$$

Equation (27) uses the sigmoid saturation function to control the size of $\rho_{ij}$, achieving a control effect where the smaller $\delta_{ij}$, the smaller $\rho_{ij}$. According to the maneuverability of the UUV, the avoidance triggering distance is set to 60 to increase safety during collision avoidance. The numerator of Equation (28) is $\delta_{ij} - 50$, and when it is around 50, the value of $\rho_{ij}$ will have a significant change, allowing the speed to decrease rapidly. The denominator of Equation (28) is set to 5 to control the speed of change in the interval. $\alpha_{u1}$ affects the speed change when the distance is too close; $\alpha_{u2}$ determines whether the speed will decrease to 0 m/s. A smaller $\alpha_{u2}$ will reduce the upper and lower limits of $\rho_{ij}$ , thereby reducing the minimum value after deceleration, but the speed cannot drop to 0 m/s to prevent the UUV from losing maneuverability and causing the avoidance action to fail.

In Equation (28), the size of $\alpha_{u3}$ controls the degree of final deceleration; $\alpha_{u4}$ determines the speed of deceleration, and a larger value results in faster deceleration. The sizes of $\alpha_{u3}$,$\alpha_{u4}$ are adjusted according to the dynamic characteristics of the UUV to achieve a suitable range of speed changes and quick response to speed changes. When UUVs avoid each other, the UUV that initiates avoidance decelerates to provide more time for avoidance actions and improve safety during avoidance. When evading a suspected target, the UUV reduces speed to slow its approach to the suspected target. According to the research on the dynamic characteristics of UUV objects and the need for avoidance speed control in this paper, the coefficients of the avoidance speed control law are set to $\alpha_{u1} = 20$, $\alpha_{u2} = 60$, $\alpha_{u3} = 10$ and $\alpha_{u4} = 20$.

### *3.5. Control Methods in Case of Communication Delays*

Underwater communication generally suffers from communication delays, and UUV formation control in this case is one of the studies in this paper. In the process of formation control, UUVs acquire state information from each other. In this paper, each member of the UUV formation can run its own control algorithm independently without communication with the central control, which reduces the communication volume. To further reduce the dependence on real-time communication, the control method of model prediction is proposed. When there is no communication information, each UUV predicts the position of other UUVs based on the control method in this paper. Due to the error in the prediction process, the predicted positions are corrected when communication information is received. This reduces the dependence on real-time communication and allows the formation to be controlled even when there is no communication for a while. The predicted model includes the proposed collision avoidance methods and added consistency methods, making the predicted results more in line with the actual actions of UUVs.

## 4. Simulation and Analysis

### *4.1. Simulation of Avoidance Method*

Simulation cases of formation transformation were designed to test the effectiveness of the avoidance method. A consistency protocol was added to the control system in order to increase the coordination of formation transformation.

The safe distance between UUVs is set as $\delta_{safe1} = 20$ m. Since the location of the suspected target is fixed, the safe distance between a UUV and the suspected target is set as $\delta_{safe2} = 15$ m. According to the motion characteristics of UUVs, the coefficients of avoidance speed control law are set as $\alpha_{u1} = 20$, $\alpha_{u2} = 60$, $\alpha_{u3} = 10$ and $\alpha_{u4} = 20$. The trigger distances are set as $\delta_{alert} = 60$ m and $\delta_{alertO} = 40$ m.

The distance between the aggregation points and the suspected target is set to 60 m; the distance between the detection points and the suspected target is set as 15 m. The position of the suspected target, the aggregation points and the detection points are set in Table 2. The initial state information of the UUVs is shown in Table 3. The simulation results of formation transformation are shown in Figure 10.

According to the formation transformation trajectory diagram, after UUVs have reached the aggregation points, they continue to approach the detection points. The heading curve and velocity curve show that $UUV_2$ and $UUV_3$ triggered the avoidance action during the formation transformation. The heading of the UUV group gradually stabilized under the guidance of the detection points. Finally, the UUV group reaches near the detection points and forms a detection formation. The UUV group completed the formation transformation in about 310 s.

From the curves of $\delta_{ij}$ and $\delta_{iO}$, it can be seen that after the distance of the avoidance trigger is reached, the UUV triggers the avoidance action to adjust the distance, causing the distance curve to fluctuate up and down. The UUV group consumed a long time to reach the aggregation points due to the avoidance action being triggered multiple times. At about 230 s, the avoidance function was turned off, because that was when the UUV group reached the aggregation points. Before the UUV group reached the aggregation points, the minimum distance between UUVs is 43.1 m and the minimum distance between UUVs and the suspected target is 46.7 m, so they are further than the safe distance. The speed and distance curves indicate that UUVs achieved consistency in position. The simulation results show that the UUV group successfully completed the formation transformation and approached the suspected target under the effect of the formation control strategy and avoidance method.

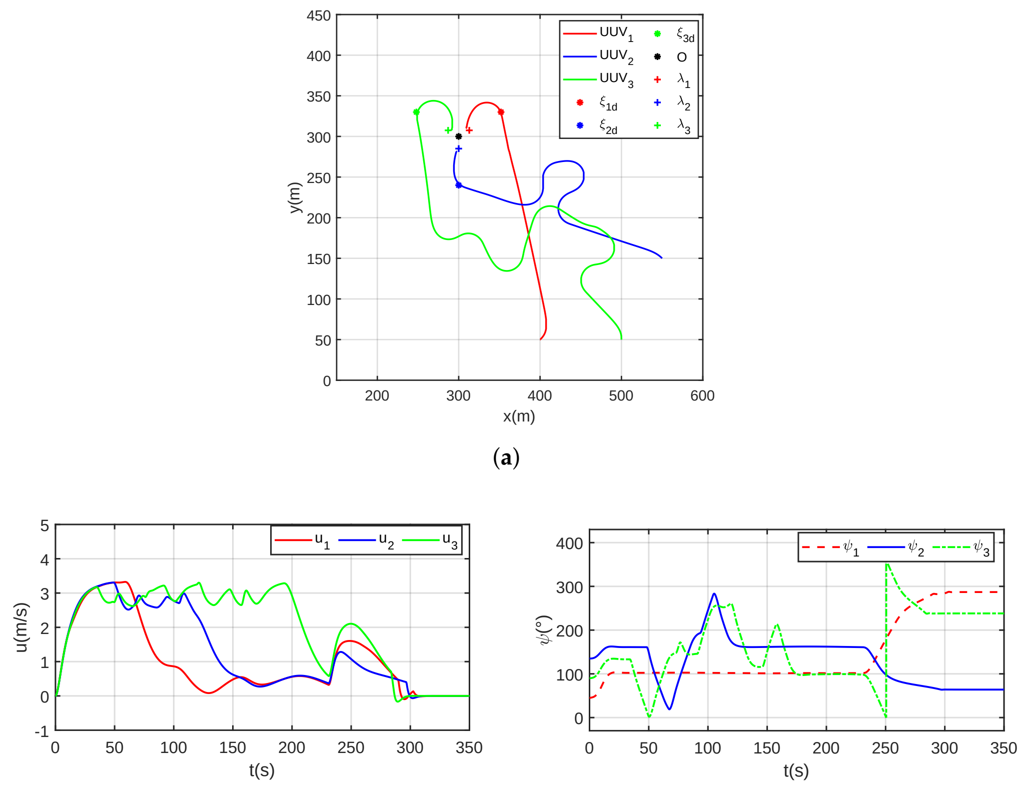


(**a**)

(**b**) (**c**)

**Figure 10.** *Cont.*

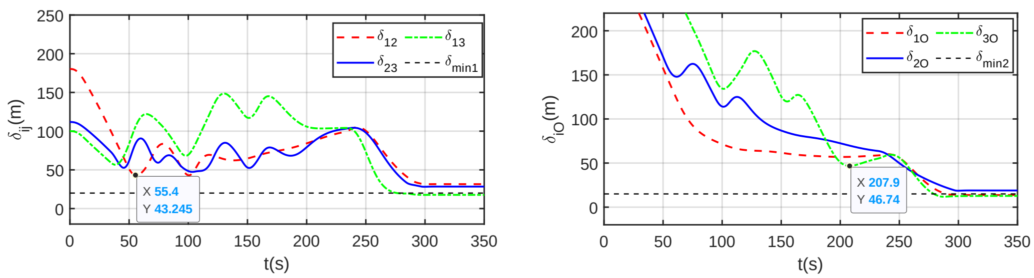


(**d**) (**e**)

**Figure 10.** UUV group formation transformation. (**a**) Position trajectory. (**b**) Velocity curve. (**c**) Heading curve. (**d**) Distance curves between UUVs. (**e**) Distance curves between UUVs and the suspected target.

**Table 2.** Position setting.

| Position \ Point | $O$ | $\xi_{1d}$ | $\xi_{2d}$ | $\xi_{3d}$ | $\lambda_1$ | $\lambda_2$ | $\lambda_3$ |
|---|---|---|---|---|---|---|---|
| $x$ (m) | 300 | 352 | 300 | 248 | 313 | 300 | 287 |
| $y$ (m) | 300 | 330 | 240 | 330 | 307.5 | 285 | 307.5 |

**Table 3.** The initial state of UUVs.

| UUV Number | $x$ (m) | $y$ (m) | $\psi$ (○) |
|---|---|---|---|
| $UUV_1$ | 400 | 50 | 45 |
| $UUV_2$ | 550 | 150 | 90 |
| $UUV_3$ | 500 | 50 | 135 |

### *4.2. Simulation of Avoidance Method*

The effectiveness of the optimal aggregation points in reducing the complexity and improving the efficiency of formation transformation is verified after the aggregation points are optimized using particle swarm.

The initial state of the UUV group and the location of the suspected target are the same as the aggregation points simulation in Section 2. When the distribution of aggregation points is $\xi_{1d} \rightarrow \xi_{3d} \rightarrow \xi_{2d} \rightarrow \xi_{1d}$, the optimization objective function has the optimal value, and the optimal solution is $\theta_1 = 179.4°$, $r_d = 60.0$ m. According to the optimal solution of the objective function, the position of the aggregation points and the detection points are shown in Table 4. The simulation results are shown in Figure 11.

**Table 4.** The position of aggregation points and detection points.

| Position \ Point | $\xi_{1d}$ | $\xi_{2d}$ | $\xi_{3d}$ | $\lambda_1$ | $\lambda_2$ | $\lambda_3$ |
|---|---|---|---|---|---|---|
| $x$ (m) | 240.0 | 330.9 | 329.1 | 285.0 | 307.7 | 307.3 |
| $y$ (m) | 301.0 | 351.4 | 247.5 | 300.3 | 312.9 | 286.9 |

The group of UUVs did not trigger avoidance actions, indicating that the distances between them and between the UUVs and the suspected target were within safe range. Since the avoidance action was not triggered, the UUVs adjusted their heading to approach the aggregation point along a straight line, and after they reached the aggregation point together, they adjusted their heading again to gradually approach the detection point. The velocity curve shows that the formation transformation was completed in about 180 s, which is a significant reduction in the time used compared to the previous simulation.

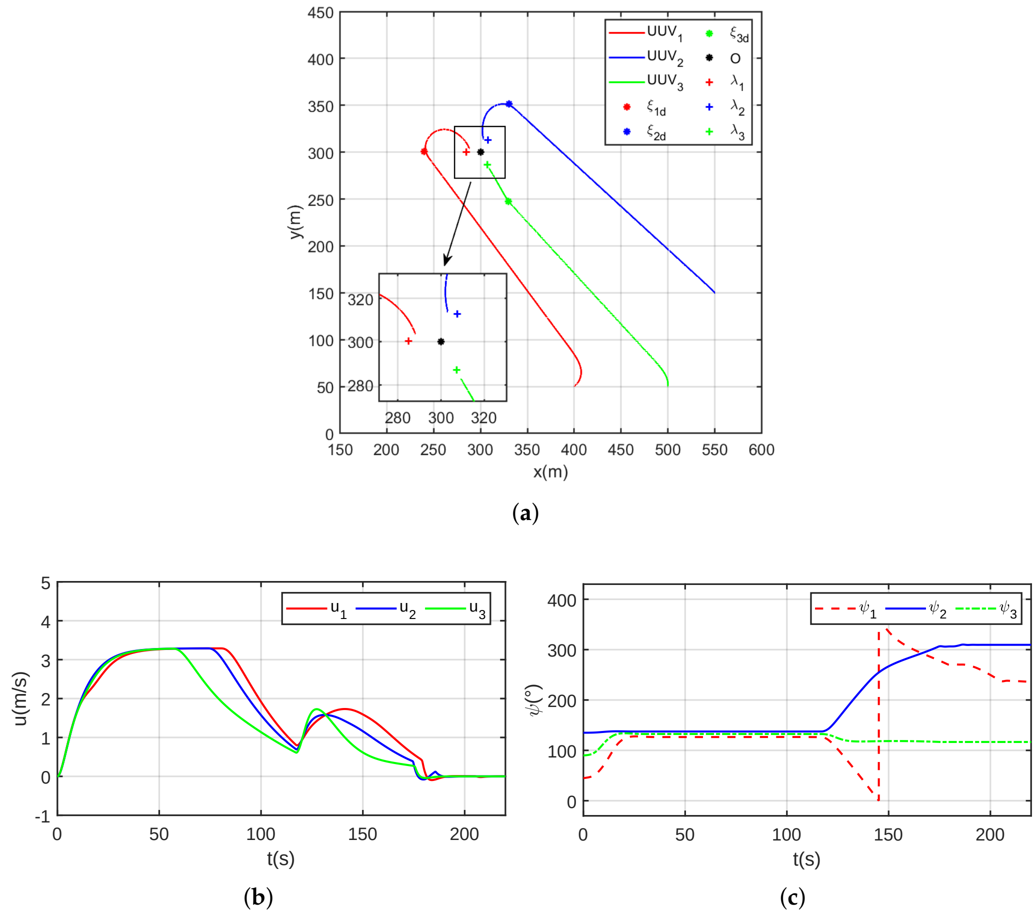


**Figure 11.** Formation transformation after aggregation position optimization. (**a**) Position trajectory. (**b**) Velocity curve. (**c**) Heading curve.

According to the analysis of the above results, after the location of the aggregation point is optimized, the trigger time of avoidance action in the process of formation transformation is reduced. The time duration of the formation transformation is shortened, and the efficiency of the formation transformation is improved.

### *4.3. Model Prediction Simulation*

Errors in the underwater position of UUVs in real-world environments arise mainly from errors in Doppler sonar-measured velocities and increase cumulatively over time. Velocity errors conforming to a normal distribution with a mean value of 10% of the measured value were added to the predicted model. Simulations of $UUV_3$ were performed when only the UUV model was predicted and there was no communication.

The simulation results of formation transformation are shown in Figure 12.

In the figure, $uuv_3$ is the actual path of $UUV_3$, and $uuv_3^1$ and $uuv_3^2$ are the predicted paths of $UUV_1$ and $UUV_2$ for $UUV_3$, which shows that there is a large error between the actual path of $UUV_3$ and the prediction of $UUV_1$ and $UUV_2$. Additionally, the longer the time, the greater the accumulation of errors.

For the next test, the UUV was set to communicate every 10 s; the simulation results of formation transformation are shown in Figure 13.

The simulation results show that the predicted paths are close to the actual paths. The following figure shows the overall path simulation.

The overall path simulation is shown in Figure 14. When communicating once every 10 s, the UUV group can still reach the expected position, and according to the speed curve, the UUV group has reached consistency. The results indicate that the proposed model prediction method can control the formation of UUVs in the case of communication delay.

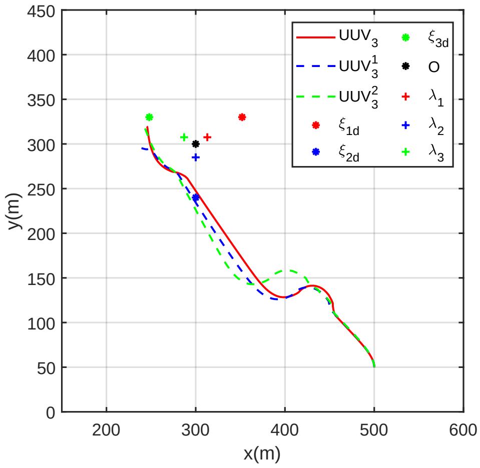


**Figure 12.** Path simulation without communication.

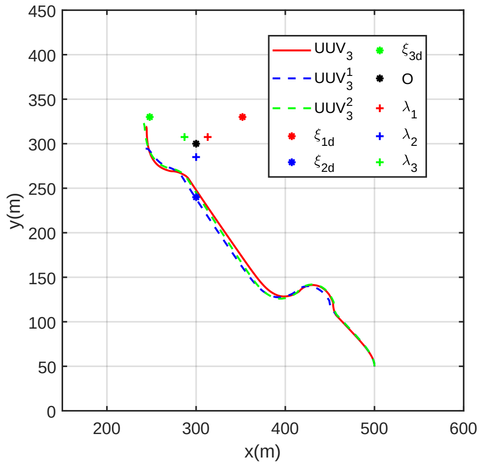


**Figure 13.** Path simulation with communication.

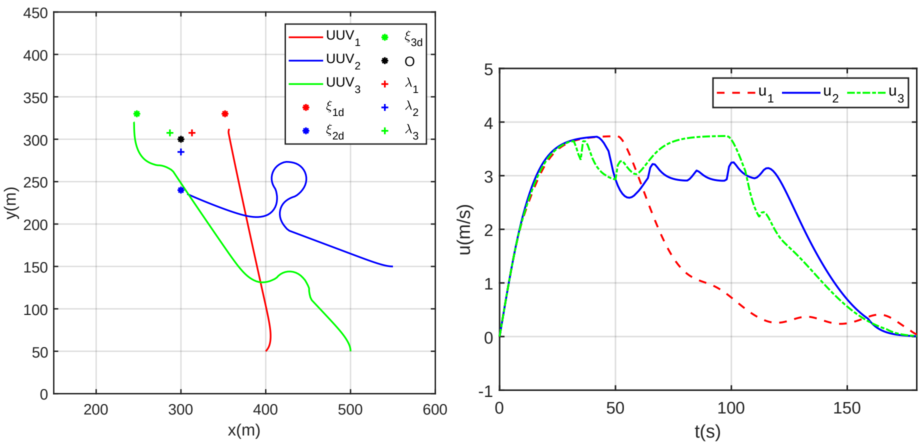


(**a**) (**b**)

**Figure 14.** Overall simulation under communication delay. (**a**) Position trajectory. (**b**) Velocity curve.

## 5. Conclusions

For the requirements of change formation to approach static targets, a formation transformation strategy is proposed. The aggregation points are used to guide the formation transformation of a UUV group, and the positions of aggregation points are optimized to improve the efficiency of formation transformation. We also decompose the position consistency into a longitudinal consistency and bow control combination, proposing the UUV longitudinal consistency protocol. Working without the need for multi-model linearization processing, simulation results show that the transformation of position consistency into longitudinal consistency is correct. In order to ensure the safety of UUVs, an avoidance method based on a virtual torque field is designed to ensure the safe distance of UUVs. The model prediction is proposed to solve the delay problem of underwater communication, and the communication results are used to correct the model prediction results. The simulation results show that the control strategy and the avoidance method all achieve the desired effect, so that the UUV group completed the formation transformation and approached the suspected target.

**Author Contributions:** L.Y.: conceptualization and writing—reviewing, methodology and editing. Z.Y.: data curation, writing—reviewing draft preparation, formal analysis, project administration, and funding acquisition. Y.H.: software, writing—original draft preparation, formal analysis, visualization, and validation. All authors have read and agreed to the published version of the manuscript.

**Funding:** This work was supported by the National Natural Science Foundation of China under Grant No. 52171303; the National Natural Science Foundation of Shandong Province under Grant No. ZR2021MF108.

**Institutional Review Board Statement:** Not applicable.

**Informed Consent Statement:** Not applicable.

**Data Availability Statement:** No new data were created or analyzed in this study. Data sharing is not applicable to this article.

**Conflicts of Interest:** The authors declare no conflict of interest.

## References

1. Liu, H.; Wang, Y.; Lewis, F.L. Robust Distributed Formation Controller Design for a Group of Unmanned Underwater Vehicles. *IEEE Trans. Syst. Man, Cybern. Syst.* **2019**, *51*, 1215–1223. [CrossRef]
2. Li, Z.; Wang, Y.; Yang, W.; Ji, Y. Development Status and Key Navigation Technology Analysis of Autonomous Underwater Vehicles. In Proceedings of the 3rd International Conference on Unmanned Systems (ICUS), Harbin, China, 27–28 November 2020; pp. 1130–1133.
3. Li, J.; Yuan, K.; Wang, H.; Da, X. Multi-AUV Fixed-point and Positioning Control Based on Virtual Leader. In Proceedings of the 16th IEEE International Conference on Mechatronics and Automation (IEEE ICMA), Tianjin, China, 4–7 August 2019; pp. 560–565.
4. Yoshida, H.; Hyakudome, T.; Ishibashi, S.; Sawa, T.; Nakano, Y.; Ochi, H.; Watanabe, Y.; Nakatani, T.; Ota, Y.; Sugesawa, M.; et al. An Autonomous Underwater Vehicle with a Canard Rudder for Underwater Minerals Exploration. In Proceedings of the 10th IEEE International Conference on Mechatronics and Automation (ICMA), Takamatsu, Japan, 4–7 August 2013; pp. 1571–1576.
5. Liang, X.; Qu, X.; Wang, N.; Zhang, R.; Li, Y. Three-Dimensional Trajectory Tracking of an Underactuated AUV Based on Fuzzy Dynamic Surface Control. *IET Intell. Transp. Syst.* **2020**, *14*, 364–370. [CrossRef]
6. Yan, Z.; Yue, L.; Zhou, J.; Pan, X.; Zhang, C. Formation Coordination Control of Leaderless Multi-AUV System with Double Independent Communication Topology and Nonconvex Control Input Constraints. *J. Mar. Sci. Eng.* **2023**, *11*, 107. [CrossRef]
7. Li, J.; Zhang, H.; Chen, T.; Wang, J. AUV Formation Coordination Control Based on Transformed Topology under Time-Varying Delay and Communication Interruption. *J. Mar. Sci. Eng.* **2022**, *10*, 950. [CrossRef]
8. Yang, Y.; Xiao, Y.; Li, T. A Survey of Autonomous Underwater Vehicle Formation: Performance, Formation Control, and Communication Capability. *IEEE Commun. Surv. Tutorials* **2021**, *23*, 815–841. [CrossRef]
9. Zhao, J.; Zhao, C.; Zhou, F. Cooperative Target Location Method Based on Master-slave Autonomous Underwater Vehicles Mobile Network. *J. Electron. Inf. Technol.* **2022**, *44*, 1919–1926.
10. Pan, X.; Yan, Z.; Jia, H.; Zhou, J.; Yue, L. Fault-Tolerant Formation Control for Multiple Stochastic AUV System under Markovian Switching Topologies. *J. Mar. Sci. Eng.* **2023**, *11*, 159. [CrossRef]
11. Yan, Z.; Xu, D.; Chen, T.; Zhang, W.; Liu, Y. Leader-Follower Formation Control of UUVs with Model Uncertainties, Current Disturbances, and Unstable Communication. *Sensors* **2018**, *18*, 662. [CrossRef]
12. Ma, S.; Wang, Y.; Zou, N.; Liang, G. A Broadband Beamformer Suitable for UUV to Detect the Tones Radiated from Marine Vessels. *Sensors* **2018**, *18*, 2928. [CrossRef]
13. Kim, J.T.; Kang, H.J.; Kim, M.K.; Hong, S.M.; Li, J.H.; Kim, M.J. Underwater Floor Pattern Matching with an Unmanned Underwater Vehicle. In Proceedings of the 12th International Conference on Ubiquitous Robots and Ambient Intelligence (URAI), Goyang, Republic of Korea, 28–30 October 2015; pp. 118–120.
14. Burlutskiy, N.; Touahmi, Y.; Lee, B.-H. Power Efficient Formation Configuration for Centralized Leader-Follower AUVs Control. *J. Mar. Sci. Technol.* **2012**, *17*, 315–329. [CrossRef]

15. Zhen, Q.; Wan, L.; Li, Y.; Jiang, D. Formation Control of a Multi-AUVs System Based on Virtual Structure and Artificial Potential Field on SE(3). *Ocean Eng.* **2022**, *253*, 111148. [CrossRef]
16. Wei, H.; Shen, C.; Shi, Y. Distributed Lyapunov-Based Model Predictive Formation Tracking Control for Autonomous Underwater Vehicles Subject to Disturbances. *IEEE Trans. Syst. Man Cybern. Syst.* **2021**, *51*, 5198–5208. [CrossRef]
17. Sun, X.; Peng, Y.; Yin, Q.; Liu, X. Multi-Agent Formation Control Based on Artificial Force with Exponential Form. In Proceedings of the 11th World Congress on Intelligent Control and Automation, Shenyang, China, 29 June–4 July 2014; pp. 3128–3133.
18. Zhang, J.; Wang, W.; Zhang, Z.; Luo, K.; Liu, J. Cooperative Control of UAV Formation Based on Distributed Consensus. In Proceedings of the IEEE 15th International Conference on Control and Automation (ICCA), Edinburgh, UK, 16–19 July 2019; pp. 788–793.
19. Yan, Z.; Zhang, C.; Tian, W.; Zhang, M. Formation Trajectory Tracking Control of Discrete-Time Multi-AUV in a Weak Communication Environment. *Ocean Eng.* **2022**, *245*, 110495. [CrossRef]
20. Li, J.; Zhang, X.; Zhang, H.; Du, X. Trajectory Tracking Control of Multi-AUVs Formation Based on Virtual Leader. In Proceedings of the 16th IEEE International Conference on Mechatronics and Automation (IEEE ICMA), Tianjin, China, 4–7 August 2019; pp. 291–296.
21. Noguchi, Y.; Maki, T. Path planning method based on artificial potential field and reinforcement learning for intervention AUVs. In Proceedings of the 2019 IEEE Underwater Technology (UT), Kaohsiung, Taiwan, 16–19 April 2019; pp. 1–6.
22. Bechlioulis, C.P.; Giagkas, F.; Karras, G.C.; Kyriakopoulos, K.J. Robust Formation Control for Multiple Underwater Vehicles. *Front. Robot.* **2019**, *6*, 90. [CrossRef]
23. Fuady, S.; Ibrahim, A.R.; Bambang, R.T. Distributed Formation Control of Multi-Robot System with Obstacle Avoidance. In Proceedings of the IEEE International Conference on Robotics, Biomimetics, and Intelligent Computational Systems (ROBIONETICS), Jogjakarta, Indonesia, 25–27 November 2013; pp. 94–98.
24. Zhang, S.; Yan, W.; Xie, G. Consensus-based leader-following formation control for a group of semi-biomimetic robotic fishes. *Int. J. Adv. Robot. Syst.* **2017**, *14*, 1729881417720784. [CrossRef]
25. Xing, W.; Shi, P.; Agarwal, R.K.; Li, L. Robust $H_\infty$ pinning synchronization for complex networks with event-triggered communication scheme. *IEEE Trans. Circuits Syst. I* **2020**, *67*, 5233–5245. [CrossRef]
26. Zhao, Y.; Xing, W.; Yuan, H.; Shi, P. A collaborative control framework with multi-leaders for AUVs based on unscented particle filter. *J. Frankl. Inst.* **2016**, *353*, 657–669. [CrossRef]
27. Yan, Z.; Zhang, C.; Tian, W.; Liu, Y. Research on Multi-AUV Cooperative Obstacle Avoidance Method During Formation Trajectory Tracking. In Proceedings of the 33rd Chinese Control and Decision Conference (CCDC), Kunming, China, 22–24 May 2022; pp. 3187–3192.
28. Meng, C.; Zhang, W.; Du, X. Finite-Time Extended State Observer Based Collision-Free Leaderless Formation Control of Multiple AUVs via Event-Triggered Control. *Ocean Eng.* **2023**, *268*, 113605. [CrossRef]
29. Yu, H.; Ning, L. Coordinated Obstacle Avoidance of Multi-AUV Based on Improved Artificial Potential Field Method and Consistency Protocol. *J. Mar. Sci. Eng.* **2023**, *11*, 1157. [CrossRef]
30. Immas, A.; Alam, M.-R. Guidance, Navigation, and Control of AUVs for Permanent Underwater Optical Networks. *IEEE J. Ocean. Eng.* **2023**, *48*, 43–58. [CrossRef]
31. Wang, L.; Zhu, D.; Pang, W.; Luo, C. A Novel Obstacle Avoidance Consensus Control for Multi-AUV Formation System. *IEEE/CAA J. Autom. Sin.* **2023**, *10*, 1304–1318. [CrossRef]
32. Zhang, W.; Wei, S.; Zeng, J.; Wang, N. Multi-UUV Path Planning Based on Improved Artificial Potential Field Method. *Int. J. Robot. Autom.* **2021**, *36*, 231–239.
33. Liu, Y.; Ding, P.; Wang, T. Autonomous Obstacle Avoidance Control for Multi-UUVs Based on Multi-beam Sonars. In Proceedings of the Global OCEANS Singapore—US Gulf Coast Conference, Biloxi, MS, USA, 5–30 October 2020.